ELSEVIER

Polymer Vol. 37 No. 10, pp. 1915–1923, 1996

0032-3861/96/$15.00+0.00

Glass transition characteristics of poly(aryl ether ketone ketone) and its copolymers

R. K. Krishnaswamy and D. S. Kalika*
Department of Chemical and Materials Engineering, University of Kentucky, Lexington, KY 40506-0046, USA
(Received 20 July 1995; revised 22 September 1995)

The glass transition characteristics of poly(aryl ether ketone ketone) (PEKK) have been investigated as a function of backbone structure and crystallization history; PEKK 100/0 homopolymer and PEKK 70/30 and 60/40 copolymers were examined, where the numbers represent the terephthalic/isophthalic (T/I) ratio. For the all-*para*-connected homopolymer, the presence of crystallinity had a significant influence on the calorimetric glass transition properties of the amorphous phase: T_g was offset by as much as 20°C in the crystallized samples as compared to the wholly amorphous material, and a sizeable ($W_{RAP} \sim 0.30$) rigid-amorphous-phase fraction was observed. In the copolymers, crystallinity had only a very minor effect on T_g. The rigid-amorphous-phase fraction in the copolymer samples was smaller as compared to the homopolymer, and was negligible ($W_{RAP} \rightarrow 0$) for samples prepared under less-restrictive crystallization conditions. Dielectric studies indicated progressive mobilization of the rigid-amorphous-phase fraction above T_g for the copolymer samples, with full mobilization of the non-crystalline fraction observed for those samples crystallized at the highest temperatures. These results show that the introduction of 1,3-connected isophthalate moieties in the PEKK copolymers has a disrupting influence on the persistence of crystalline constraint into the amorphous phase. Similar observations have been reported for poly(phenylene sulfide) copolymers and thermoplastic polyimides that incorporate *meta*-phenylene linkages in the chain backbone.

(Keywords: poly(ether ketone ketone); glass transition; dielectric relaxation)

INTRODUCTION

The nature of the non-crystalline (i.e. amorphous) regions in semicrystalline polymers is a subject of considerable interest. A broad body of experimental and theoretical literature has evolved which seeks to elucidate the influence of crystalline structure and morphology on the characteristics of this amorphous phase. One class of polymers that has received significant attention in this regard are 'low-crystallinity' polymers (see designations presented by Boyd[1]). These are typically semiflexible polymers containing aromatic groups in the chain backbone. The semiflexible nature of these materials leads to relatively slow crystallization rates such that they can be quenched from the melt to a wholly amorphous glass. The ability to obtain a wholly amorphous sample is important in that it provides a reference material in which no crystallinity is present, thereby facilitating comparative studies of the amorphous phase with crystallized samples of controlled history. Examples of low-crystallinity thermoplastics include poly(ethylene terephthalate) (PET), poly(phenylene sulfide) (PPS) and poly(ether ether ketone) (PEEK).

The presence of crystallinity in these polymers leads to the constraint of amorphous chain mobility in the vicinity of the glass transition. This is manifested by a positive offset of the order of 10–20°C in the glass transition temperature of the semicrystalline specimens as compared to their wholly amorphous counterparts, as well as a broadening of the glass transition (see results for PET[1–3], PPS[4–6], PEEK[7–11]). For the semicrystalline samples, the measured glass transition temperature is observed to decrease with less-restrictive crystallization conditions. Cold crystallization at progressively higher temperatures, for example, leads to a systematic decrease in T_g, although the glass transition temperature for all crystallized samples is still well above that measured for the quenched material. This trend demonstrates that the degree of constraint imposed by the crystallites on the amorphous-phase motions is a sensitive function of crystallization history and the corresponding morphology that develops. Crystallization at conditions of relatively high chain mobility and low nucleation density leads to a morphology that imposes less constraint on the motion of the amorphous chains. This loosening of the crystalline constraint has been attributed to improved crystal perfection (i.e. a decrease in lamellar surface roughness[5]) as well as thickening of the amorphous interlayer[3,11].

In addition to the observed offset in glass transition temperature, the presence of crystallinity leads to a disproportionate decrease in the magnitude of the glass transition for these materials. Calorimetric studies reveal that the incremental step change in heat capacity at the glass transition, $\Delta C_p(T_g)$, is reduced to a much greater degree than would be anticipated based simply on the

* To whom correspondence should be addressed

immobilization of those chains incorporated into the crystalline phase. This result is consistent with a persistence of order into the nominally amorphous material which can be quantified in terms of a rigid-amorphous-phase fraction (W_{RAP}), where W_{RAP} represents all non-crystalline material that remains immobile across the glass transition. Early studies of the rigid amorphous phase by Wunderlich and coworkers examined semicrystalline poly(oxymethylene)s[12,13] and polypropylene[14]. Recent studies have reported sizeable rigid-amorphous-phase fractions in both PPS[4–6] and PEEK[7,8]. In the case of the PPS and PEEK investigations, the amount of rigid amorphous material measured for a given sample varied with the thermal history in a manner consistent with the T_g results cited above. Less-restrictive crystallization conditions (e.g. higher cold-crystallization temperatures, or slow cooling from the melt) led to a reduction in the amount of rigid amorphous phase present. Dielectric studies on these two semiflexible polymers indicated a progressive mobilization of some portion of the rigid-amorphous-phase fraction with increasing temperature in the range between T_g and crystalline melting[8,9,15,16].

As described above, the influence of crystallinity on the glass-rubber relaxation characteristics of semiflexible, thermally resistant thermoplastics such as PPS and PEEK has been examined in detail. Although these studies explore a wide range of thermal histories and corresponding semicrystalline morphologies, they are limited in that the possible influence of polymer backbone structure is not addressed. In fact, relatively minor modifications in the structure or connectivity of these semiflexible polymers can lead to significant changes in the crystallization and melting behaviour of the materials, and thus provide a means by which to tailor the polymers for improved processability. The incorporation of low levels of 1,3-connected *meta*-phenylene linkages into the all-*para* backbones of poly(phenylene sulfide)[6,17] and poly(aryl ether ketone)s[18] has been shown to produce a substantial reduction in equilibrium melting temperature, with only a modest impact on the measured glass transition temperature. Recent studies in our laboratory have assessed the influence of varying levels of *meta*-phenylene content on the glass transition characteristics of PPS as related to crystalline morphology[6,16]. It was observed that the introduction of 5–10% *meta* linkages in the PPS backbone led to a considerable loosening of the constraints imposed by the crystal lamellae on the relaxation of the amorphous chains. Specifically, the offset in T_g relative to the amorphous samples was diminished with increasing *meta* content. Also, dielectric studies revealed virtually full mobilization of the rigid-amorphous-phase fraction at temperatures just above the glass transition for those samples containing 8% and 10% *meta*-phenylene units. It was speculated that the majority of the *meta*-phenylene defects were excluded to the crystal lamellar surface in the copolymer samples, where they acted to disrupt the persistence of order into the amorphous phase.

In the work reported here, the glass transition characteristics of a series of poly(aryl ether ketone ketone) (PEKK) polymers are investigated as a function of backbone structure and thermal history. The PEKK polymers are the result of the polycondensation of diphenyl ether and isophthalic (I) and terephthalic (T) acids (see structure). The presence of the *meta*-connected

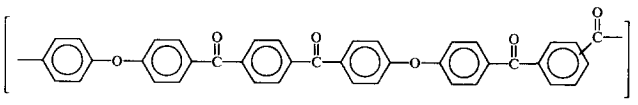

T T/I

isophthalate moiety leads to a large reduction in melting temperature and a modest decrease in glass transition temperature with increasing isophthalate content[18]; this latter effect is attributed to an increase in overall chain flexibility with the introduction of the *meta* linkages. The compositions examined here include the PEKK 100/0 (T/I) homopolymer, and two copolymer compositions, PEKK 70/30 and PEKK 60/40. Both calorimetric and dielectric methods are used to elucidate the influence of crystallinity on the glass transition of these materials as a function of isophthalate content and crystallization condition. As will be demonstrated, the relaxation characteristics of the PEKK copolymers are largely analogous to those observed for the modified PPS samples: the incorporation of *meta*-phenylene segments leads to a loosening of the constraints imposed by the crystallites on the amorphous-phase motions and disruption of the rigid amorphous phase.

MATERIALS AND EXPERIMENTAL METHODS

PEKK polymers with terephthalic/isophthalic (T/I) ratios of 100/0, 70/30 and 60/40 were provided through the courtesy of E. I. DuPont de Nemours. Amorphous films (0.13 and 0.38 mm thickness) were prepared by compression moulding the as-received pellets at their respective thermodynamic melting temperatures (see ref. 18) for approximately 4 min, followed by quenching in ice–water. The quenched samples displayed no crystalline order as determined by X-ray measurements. Cold-crystallized samples were prepared by isothermally annealing the quenched films at designated temperatures in the Carver melt press for a period of 3 h. Melt-crystallized films were prepared by equilibrating the PEKK pellets at their thermodynamic melting temperature for 4 min in the melt press, followed by direct transfer of the isotropic melt to a second press held at the desired crystallization temperature. The samples were subsequently annealed at that temperature for 3 h. Cold-crystallization temperatures were in the range 200–300°C (PEKK 100/0 and PEKK 70/30) and 200–275°C (PEKK 60/40). Melt-crystallization temperatures were in the range 280–300°C (PEKK 70/30) and 240–270°C (PEKK 60/40). The thinner (0.13 mm) films were used for both X-ray and dielectric measurements, while the thicker (0.38 mm) films were employed in the calorimetric experiments. All samples were vacuum dried at 50°C for at least 24 h prior to measurement.

Wide-angle X-ray scattering (WAXS) was employed to assess the degree of crystallinity in all samples. Samples were examined using a Rigaku X-ray diffractometer with Cu K_α radiation at room temperature across a range of scattering angles (2θ) from 5° to 45°; the scan rate was 2° min^{-1} with a data interval of 0.02°. For each composition, the diffraction pattern from a corresponding amorphous quenched film was scaled and subtracted from the semicrystalline result; it was assumed that the scattering of the amorphous segments in the semicrystalline specimens could be represented by the scattering

halo of the corresponding amorphous films. The degree of crystallinity was estimated as the ratio of the net crystalline scattering intensity to the overall scattering intensity.

Calorimetric studies were performed using the Perkin-Elmer DSC-7 differential scanning calorimeter. Transition temperatures and melting enthalpy were calibrated using indium and zinc standards. A sapphire reference was used for the calibration of heat capacity. All scans were performed under an inert (N_2) atmosphere at a scanning rate of 20°C min^{-1}.

The heat-capacity increment across the glass transition for the amorphous PEKK copolymers was determined via extrapolation of the measured solid and liquid heat capacity–temperature relations. Solid-state heat capacities were determined across a temperature range of 50–120°C for all compositions. Liquid heat-capacity measurements were performed across a temperature range of 330–370°C for PEKK 70/30 and 330–360°C for PEKK 60/40; these measurements were obtained by heating the samples above their respective equilibrium melting temperatures, with supercooling into the range of interest. The heat capacity–temperature relations were found to be linear across both temperature ranges, and in the case of the 70/30 and 60/40 copolymers, the extrapolated values were in excellent agreement with $\Delta C_p(T_g)$ measured directly from non-isothermal heating scans of the quenched specimens. Liquid heat-capacity measurements for the PEKK 100/0 composition were not reproducible, possibly due to thermal degradation at the high temperatures required. Therefore, for the 100/0 composition, the heat-capacity increment at T_g was taken as the measured value based on a non-isothermal scan of the quenched material. The heat-capacity measurements were consistent over multiple runs; the reported values represent averages for at least five samples per composition.

Dielectric spectroscopy measurements were accomplished using a Polymer Laboratories Dielectric Thermal Analyzer (PL-DETA) comprised of a GenRad Digibridge interfaced with the Polymer Laboratories temperature controller. Concentric silver electrodes (33 mm) were vacuum evaporated directly on the samples, which were mounted between polished platens in the temperature-controlled test oven; all measurements were carried out under an inert (N_2) atmosphere. The dielectric constant (ϵ') and loss factor ($\tan\delta$) were recorded at frequencies ranging from 50 Hz to 100 kHz across a temperature range of 50–300°C; the heating rate was 1°C min^{-1}.

RESULTS AND DISCUSSION

Quenched samples

PEKK samples quenched from the melt were found to be wholly amorphous as indicated by X-ray diffraction measurements; only an amorphous halo was observed for the PEKK compositions examined here. The calorimetric glass transition characteristics of the quenched PEKK films are presented in *Table 1*. The reported T_g is taken as the midpoint of the incremental step change in heat capacity for heating scans performed at 20°C min^{-1}. The amorphous T_g values measured for the two copolymer compositions (PEKK) 70/30 and PEKK 60/40) are in good agreement with values originally reported by Gardner *et al.*[18] The glass transition temperature measured for the amorphous PEKK 100/0 homopolymer is somewhat lower than that reported in the literature, such that a systematic variation in T_g with isophthalate content is not strictly observed.

Measurement of the heat capacity as a function of temperature for the solid quenched polymer and in the liquid melt revealed linear relations, which could be extrapolated to T_g in order to establish the incremental change in heat capacity for the amorphous material; these values are reported for the copolymers in *Table 1*. The extrapolated values determined for the PEKK copolymers are very similar to that reported for PEEK[7], and are in close agreement with ΔC_p measured directly from non-isothermal heating scans of the quenched specimens. This latter result provides additional evidence as to the wholly amorphous nature of the quenched films. For the PEKK 100/0 homopolymer, thermal degradation at long times in the melt precluded the reliable determination of liquid heat capacity as a function of temperature. The value of ΔC_p reported in *Table 1* for the PEKK homopolymer is based on a non-isothermal heating scan of the quenched material (20°C min^{-1}).

Crystal structure and morphology

The crystal structure and morphology that are observed for the PEKK polymers are a function of both backbone composition and the conditions of crystallization. PEKK is polymorphic in nature, in that multiple crystal unit-cell structures are observed depending upon the flexibility of the polymer chain and molecular mobility under the crystallization conditions; polymorphism in poly(aryl ether ketone)s has been investigated in detail by Gardner *et al.*[18,19] and in collaboration with Cheng and coworkers[20–22]. The polymorphic nature of these samples leads to a complicated melting behaviour, as crystal reorganization occurs during sample heating[18,22]. As a result, it is difficult to establish the degree of crystallinity in these materials based on the measured heat of fusion as determined via calorimetric measurements. For the work reported here, we have used X-ray diffraction in order to obtain unambiguous, room-temperature determinations of the degree of crystallinity (W_C) in the various semicrystalline specimens. These measurements not only provide reliable values of W_C, but offer additional insight as to the existence of multiple crystal forms as a function of backbone structure and thermal history.

The degree of crystallinity determined for the PEKK homopolymer and copolymers is reported as a function of crystallization temperature in *Table 2*. The observed trends are consistent with previous studies on semiflexible polymers such as PPS[4–6] and PEEK[7–10]: a systematic increase in W_C is observed with increasing

Table 1 Calorimetric glass transition properties of amorphous PEKK 100/0 homopolymer and PEKK 70/30 and PEKK 60/40 copolymers

	T_g (°C)	ΔC_p (J g^{-1} $°C^{-1}$)
PEKK 100/0	156.1	0.26[a]
PEKK 70/30	159.6	0.29
PEKK 60/40	157.9	0.27

[a] ΔC_p for 100/0 composition based on non-isothermal scan of quenched material (20°C min^{-1})

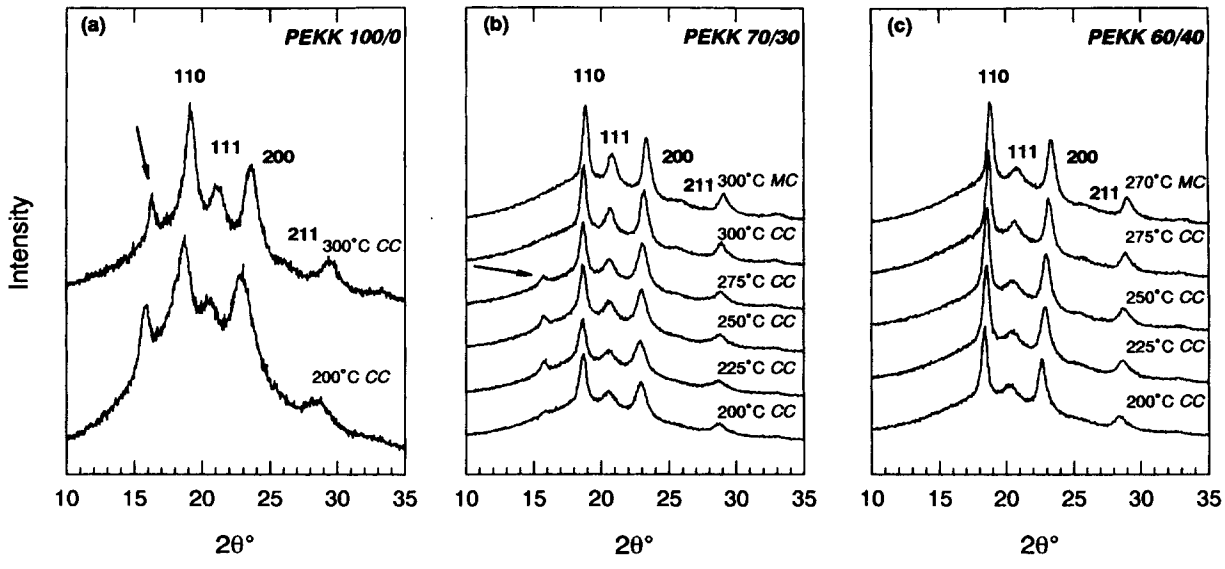

Figure 1 Wide-angle X-ray diffraction patterns, i.e. intensity vs. 2θ (deg), for PEKK homopolymer and copolymers: (a) PEKK 100/0; (b) PEKK 70/30; (c) PEKK 60/40. Cold-crystallization (CC) or melt-crystallization (MC) temperatures as indicated

crystallization temperature, with higher levels of overall crystallinity observed for crystallization from the melt. The degree of crystallinity in the copolymers is lower than that of the PEKK 100/0 homopolymer, and decreases with increasing *meta* content for these two copolymer compositions.

X-ray diffraction patterns across the range of thermal histories are reported for the homopolymer and PEKK 70/30 and 60/40 copolymers in *Figure 1*. In all cases, the diffraction pattern is dominated by reflections at $2\theta \sim 18.7°$ (1 1 0), 20.8° (1 1 1), 23.3° (2 0 0) and 29.0° (2 1 1). These reflections correspond to the form I structure, and are in good agreement with values reported previously[20]; the reflection peak positions are indexed according to a two-chain orthorhombic unit cell with two phenylene units per repeat in the *c*-axis direction. The appearance of a second structure, as originally reported by Blundell and Newton[23], is observed for poly(aryl ether ketone)s with relatively stiff backbone structures, or under highly restrictive crystallization conditions (e.g. solvent crystallization). For the samples examined here, the coexistence of the form II structure with the dominant form I is manifested by an additional diffraction peak at ~15.8°, which corresponds to the (0 2 0) reflection of the form II two-chain orthorhombic unit cell. The appearance of the (0 2 0) reflection in the diffraction patterns reported in *Figure 1* is indicated by an arrow. In agreement with the previous studies of polymorphism for these polymers, we observe the most prominent coexistence of the form II structure for the PEKK 100/0 homopolymer, which has the stiffest chain backbone of the compositions examined; note that the 'pure' form II structure can only be obtained via solvent crystallization. The introduction of *meta*-phenylene units into the chain backbone leads to an increase in overall chain flexibility, and thus a reduction in the relative population of form II crystals. Examination of the diffraction patterns for the PEKK 70/30 copolymer reveals a small (0 2 0) reflection at ~15.8°, which weakens and eventually disappears as the crystallization conditions become less restrictive (i.e. higher crystallization temperatures). For the PEEK 60/40 copolymer, no form II reflections are evident.

Calorimetric glass transition

The glass transition temperatures of the crystallized PEKK polymers as determined by d.s.c. are reported as a function of crystallization temperature in *Table 2*. Examination of the results for the PEKK 100/0 homopolymer reveals a significant positive offset in glass transition temperature for the cold-crystallized specimens as compared to the wholly amorphous sample; the offset in T_g, namely $\Delta T_g = T_g^{SC} - T_g^{A}$, is nearly 20°C for the sample cold crystallized at 200°C, and decreases with increasing annealing temperature. These data are fully consistent with results reported for other semiflexible, low-crystallinity homopolymers such as PET, PPS and PEEK (see discussion, above). The offset in T_g reflects the constraints imposed by the crystallites on the large-scale amorphous-chain motions inherent to the glass transition. As the crystallization conditions become less restrictive, the constraint is loosened to some extent.

Examination of the results for the PEKK 70/30 and 60/40 copolymers shows that the presence of isophthalate moieties in the chain backbone leads to a considerable reduction in the level of constraint imposed by the crystal structure on the glass–rubber relaxation. For the 70/30 T/I copolymer composition, ΔT_g is only 3.5°C for the most-restrictive crystallization condition (cold crystallization at 200°C); the offset in T_g is negligible for higher cold-crystallization temperatures and crystallization from the melt. This effect is even more pronounced for the 60/40 copolymer composition, where only a 2°C offset in T_g is observed at the most-restrictive cold-crystallization condition. Here again, ΔT_g is negligible for higher crystallization temperatures.

The glass transition results obtained for the PEKK all-*para* homopolymer and copolymers are consistent with trends observed for PPS copolymers incorporating up to 10% *meta*-phenylene linkages[6,16]. The introduction of increasing *meta* content in the PPS backbone led to a systematic reduction in ΔT_g: ΔT_g had a value of only

2–3°C for 10% PPS copolymers melt crystallized at higher temperatures. In the PPS studies, wide-angle X-ray measurements suggested that the majority of the *meta*-phenylene chain defects were excluded to the crystal lamellar surface, where they acted to disrupt the constraining influence of the crystallites on the amorphous segments. For the PEKK copolymers, WAXS studies by Gardner *et al.*[18] also indicated a high degree of defect exclusion for the 70/30 T/I composition. X-ray measurements for PEKK 60/40, however, indicated nearly complete inclusion, with the crystalline phase comprised of terephthalic–isophthalic diads.

The above discussion attributes the difference in crystalline constraint observed for the PEKK copolymers as compared to the homopolymer to a structural effect, namely the presence of *meta*-phenylene defects in the vicinity of the crystal–amorphous boundary. One other significant consideration in this regard is the crystallization kinetics that are operative at a particular crystallization condition, and the influence of the kinetics on crystal perfection and the corresponding constraint imposed on amorphous-chain motions. The introduction of isophthalate units in the PEKK backbone has a dramatic effect on crystallization kinetics, with the presence of the isophthalate segments leading to a strong decrease in crystallization rate[18]. At a given crystallization temperature, this would result in a significantly lower degree of crystal perfection in a homopolymer specimen, for example, as compared to the copolymers; lower degrees of crystal perfection (i.e. greater lamellar surface roughness) have been correlated with a higher degree of crystalline constraint and a correspondingly greater offset in T_g (ref. 5). The offset in T_g for a copolymer sample, by comparison, would be lower owing to the higher degree of lamellar perfection that presumably develops. The glass transition results reported above for the PEKK polymers most likely reflect the influence of both the backbone structural effect and crystallization rate. In the case of the PPS copolymers[6], the influence of *meta* content on T_g independent of crystallization rate was conclusively demonstrated by comparing ΔT_g for the various copolymer compositions at approximately the same crystallization rates. A similar comparison based on the PEKK data reported here is not feasible owing to the vast difference in crystallization rate inherent to the PEKK 100/0 homopolymer as compared to the two copolymers.

Rigid amorphous phase

The glass transition measurements show that there is a strong correlation between the presence of isophthalate units in the PEKK chain backbone and the degree of constraint imposed by the crystallites on the motions of the amorphous phase. Given the influence of polymer backbone composition on the apparent disruption of order at the lamellar surface, it is of interest to assess possible variations in rigid-amorphous-phase fraction in these materials as a function of isophthalate content and thermal history.

When considered on a calorimetric basis, the rigid-amorphous-phase fraction is identified as that portion of the non-crystalline material that does not contribute to the observed increase in heat capacity across the glass transition, and thus remains frozen at T_g. If the mobile amorphous fraction is defined as:

$$W_{MA} = \Delta C_p^{SC} / \Delta C_p^{A} \quad (1)$$

where ΔC_p^{SC} corresponds to the measured increase in heat capacity for the semicrystalline sample and ΔC_p^{A} corresponds to the extrapolated heat-capacity increase for a wholly amorphous sample, than the rigid-amorphous-phase fraction (W_{RAP}) can be calculated from the difference:

$$W_{RAP} = 1 - W_{MA} - W_C \quad (2)$$

where W_C represents the degree of crystallinity determined from independent WAXS measurements.

The application of the three-phase model to the PEKK 100/0 homopolymer is reported in *Table 2a*. The PEKK homopolymer displays a significant rigid-amorphous-phase fraction ($W_{RAP} \sim 0.30$), which is independent of cold-crystallization temperature. This level of rigid amorphous phase is comparable to that reported for the PPS[5,6] and PEEK[8] homopolymers. However, the gradual decrease in rigid-amorphous-phase fraction that is typically observed with increasing crystallization temperature is not evident in this case.

Phase determinations for the PEKK 70/30 and 60/40 copolymers are reported in *Tables 2b* and *2c*, respectively. The two copolymers display W_{RAP} values that are lower than that observed for the PEKK homopolymer and decrease with increasing crystallization temperature; W_{RAP} is essentially zero at the highest crystallization temperatures examined. These results demonstrate the sensitivity of the rigid-amorphous-phase fraction to the conditions of crystallization and also the disruption of the rigid amorphous phase with the introduction of isophthalate units into the chain backbone. The gradient of immobilization at the crystal surface that corresponds to the rigid amorphous phase is evident in the PEKK copolymers only at the most-restrictive crystallization conditions (i.e. lowest cold-crystallization temperatures). For less-restrictive crystallization conditions, the isophthalate linkages are sufficient to disrupt any persistence of order into the amorphous phase, such that the measured value of W_{MA} is in direct proportion to the total population of non-crystalline material.

Dielectric glass transition

Dielectric spectroscopy provides a sensitive means by which to elucidate further the characteristics of the glass transition by probing the mobility of the constituent dipoles of the polymer chains as a function of test frequency and temperature. Dielectric measurements have been particularly effective in tracking the potential relaxation of rigid-amorphous-phase material in semi-flexible polymers at temperatures between T_g and crystalline melting. Studies on semicrystalline PPS[15,16] and PEEK[8,9] showed a progressive increase in dielectric relaxation intensity with increasing temperature above T_g, which was attributed to a gradual mobilization of some portion of the rigid-amorphous-phase fraction prior to melting. For the PEKK studies described here, dielectric measurements serve as an additional method by which to assess the influence of varying backbone structure on the glass transition and the possible disruption of the rigid amorphous phase.

Table 2 Calorimetric and dielectric characteristics of PEKK homopolymer and copolymers as a function of isothermal crystallization temperature. T_g (°C) = calorimetric glass transition temperature; T_α (°C) = dielectric glass transition temperature based on maximum in dielectric loss at 1 kHz; W_C = degree of crystallinity based on WAXS; W_{MA} = mobile-amorphous-phase fraction; W_{RAP} = rigid-amorphous-phase fraction. CC, cold crystallization; MC, melt crystallization

(a) PEKK 100/0

Thermal history	T_g (°C)	W_C (±0.02)	W_{MA} (±0.01)	W_{RAP} (±0.03)
200°C, CC	175.9	0.32	0.39	0.29
250°C, CC	173.8	0.39	0.31	0.30
300°C, CC	169.9	0.43	0.27	0.30

(b) PEKK 70/30

Thermal history	T_g (°C)	T_α (°C)	W_C (±0.02)	W_{MA} (±0.01)	W_{RAP} (±0.03)
Amorphous	159.6	164.4	–	–	–
200°C, CC	163.1	176.4	0.28	0.48	0.24
225°C, CC	162.8	168.9	0.29	0.52	0.19
250°C, CC	160.3	165.3	0.31	0.55	0.14
275°C, CC	159.6	165.1	0.37	0.62	0.01
300°C, CC	159.8	164.9	0.36	0.66	<0
280°C, MC	159.4	166.3	0.35	0.62	0.03
300°C, MC	159.5	165.4	0.38	0.66	<0

(c) PEKK 60/40

Thermal history	T_g (°C)	T_α (°C)	W_C (±0.02)	W_{MA} (±0.01)	W_{RAP} (±0.03)
Amorphous	157.9	160.2	–	–	–
200°C, CC	159.8	169.3	0.22	0.52	0.26
225°C, CC	159.6	169.8	0.26	0.56	0.18
250°C, CC	158.1	166.9	0.32	0.63	0.05
275°C, CC	158.0	163.8	0.34	0.70	<0
240°C, MC	158.5	167.8	0.34	0.56	0.10
270°C, MC	157.7	160.9	0.35	0.67	<0

Dielectric results for amorphous PEKK 70/30 are reported as isochronal plots of dielectric constant (ϵ') and dielectric loss ($\epsilon'' = \epsilon' \tan\delta$) *versus* temperature in *Figure 2*. Examination of the dielectric constant shows a strong, stepwise increase in ϵ' starting at 150°C, which corresponds to large-scale mobilization of the amorphous chains, i.e. the glass–rubber (α) relaxation; this is accompanied by a narrow peak in dielectric loss. The abrupt, frequency-independent decrease in dielectric constant that is observed at ~180°C corresponds to the onset of cold crystallization in the non-isothermal scan, as some fraction of the responding dipoles are immobilized by the evolving crystalline structure. The presence of crystallinity leads to a broadening of the α relaxation, and the eventual mobilization of the remaining amorphous material at higher temperatures (>185°C) is evident as a gradual increase in ϵ' and a broad shoulder on the high-temperature side of the glass transition loss peak.

Dielectric data for a representative cold-crystallized sample (PEKK 70/30, cold crystallized at 250°C) are shown in *Figure 3*. In this case, a single incremental increase in dielectric constant is observed at the glass transition, which is not complicated by the effects of crystallization during the scan. The dielectric loss peak for the crystallized sample is considerably broadened as compared to the wholly amorphous specimen, as the responding chains experience a much wider spectrum of local relaxation environments. The observed increase in dielectric constant and loss at lower test frequencies and higher temperatures corresponds to the onset of ionic conductivity. The influence of conductivity on the dielectric loss data was removed prior to analysis by the method outlined in ref. 24.

Dielectric glass transition temperatures (T_α, 1 kHz) based on the maximum in dielectric loss are reported for the amorphous and crystallized PEKK copolymer samples in *Table 2*. The trends observed in the dielectric data are consistent with the calorimetric studies, although a stronger positive offset in transition temperature with the presence of crystallinity is observed for the dielectric results; this behaviour suggests that the dielectric probe is somewhat more sensitive to the constraining influence of crystallinity in these samples as compared to the calorimetric measurements. T_α decreases with increasing crystallization temperature, and approaches the amorphous-specimen value at the highest crystallization temperatures examined.

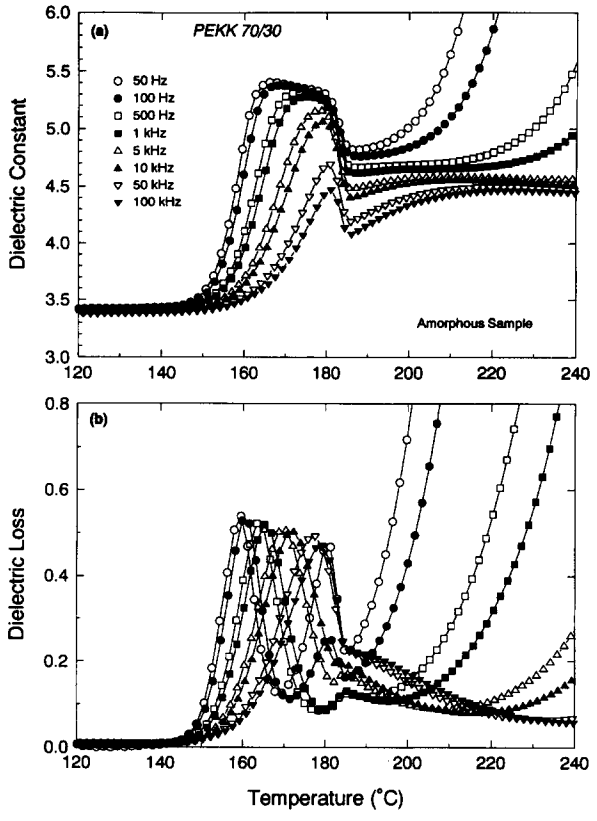

Figure 2 Dielectric results for amorphous PEKK 70/30 copolymer: (a) dielectric constant (ϵ') vs. temperature (°C); (b) dielectric loss (ϵ'') vs. temperature (°C). Symbols: (○) 50 Hz, (●) 100 Hz, (□) 500 Hz, (■) 1 kHz, (△) 5 kHz, (▲) 10 kHz, (▽) 50 kHz, (▼) 100 kHz

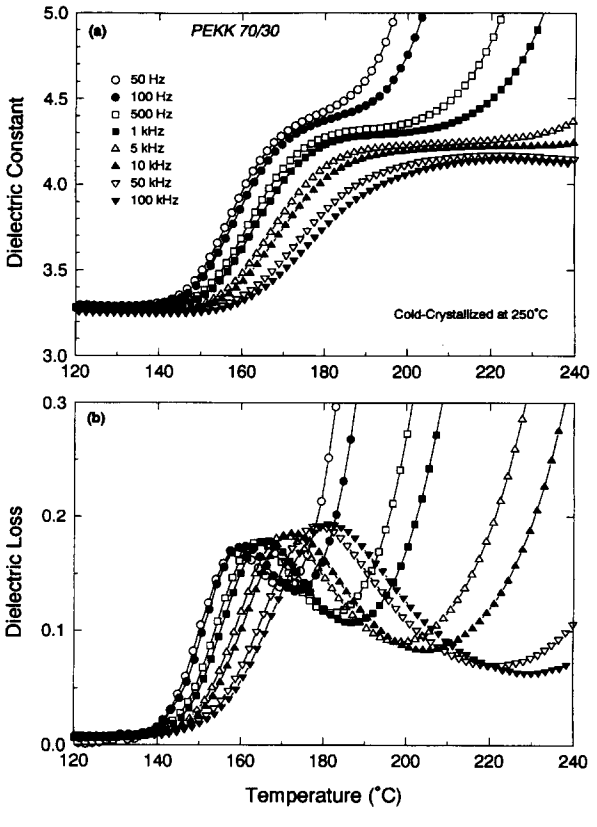

Figure 3 Dielectric results for PEKK 70/30 copolymer cold crystallized at 250°C: (a) dielectric constant (ϵ') vs. temperature (°C); (b) dielectric loss (ϵ'') vs. temperature (°C). Symbols: (○) 50 Hz, (●) 100 Hz, (□) 500 Hz, (■) 1 kHz, (△) 5 kHz, (▲) 10 kHz, (▽) 50 kHz, (▼) 100 kHz

The time–temperature characteristics of the dielectric α relaxation are presented as Arrhenius plots of log (frequency) *versus* reciprocal temperature ($1000/T_{max}$) in *Figure 4*; T_{max} is based on the maximum in the isochronal dielectric loss curves. Data are provided for the wholly amorphous samples, and specimens crystallized at the extremes of the cold-crystallization range. Each data set can be satisfactorily described using a WLF (Williams–Landel–Ferry) expression across the range of frequencies examined[25], with the offset in the various curves indicative of the relatively modest constraint imposed by the crystals on the amorphous-phase relaxation. The apparent activation energy, which corresponds to the slope of the log(frequency) *versus* $1/T$ curves, appears insensitive to copolymer backbone composition and crystalline morphology.

The dielectric dispersion in the vicinity of the glass–rubber relaxation was analysed for the PEKK copolymer samples using the Havriliak–Negami modification of the single-relaxation-time Debye expression[26]:

$$\epsilon^* = \epsilon_U + \frac{\epsilon_R - \epsilon_U}{[1 + (i\omega\tau)^{\beta}]^{\alpha}} \quad (3)$$

where ϵ_R and ϵ_U represent the relaxed ($\omega \to 0$) and unrelaxed ($\omega \to \infty$) values of the dielectric constant, ω is the frequency, τ is the central relaxation time, and β and α represent the broadening and skewing parameters, respectively. Results for the PEKK 70/30 copolymer are presented below.

Argand plots of dielectric loss (ϵ'') *versus* dielectric constant (ϵ') were constructed at selected temperatures in the glass transition region for the amorphous and cold-crystallized samples; representative results for the PEKK

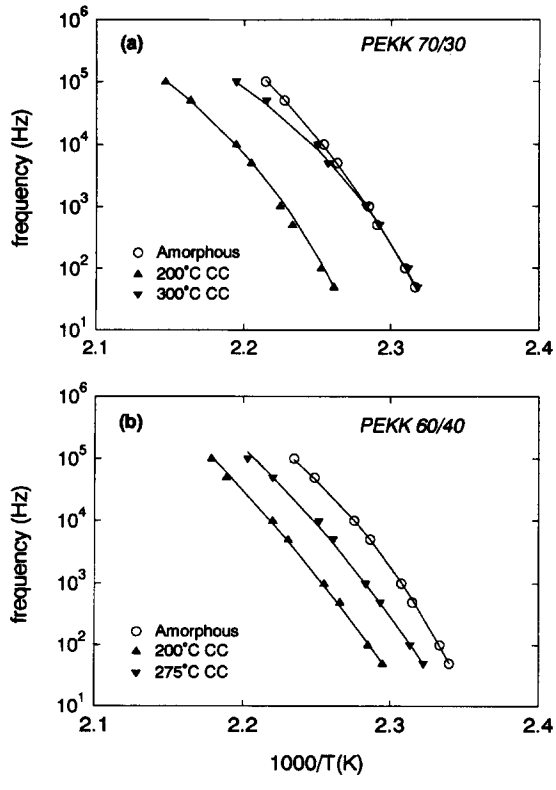

Figure 4 Arrhenius plots of dielectric test frequency (Hz) vs. $1000/T_{max}$ (K^{-1}) based on isochronal temperature sweeps, for amorphous and cold-crystallized specimens: (a) PEKK 70/30; (b) PEKK 60/40

70/30 copolymer cold crystallized at 250°C are provided in *Figure 5*. For both amorphous and crystallized specimens, the dispersion was symmetric and was described by the Cole–Cole form of equation (3), with α, the skewing parameter, equal to unity[27]. By performing least-squares fits to the Argand plots, the Cole–Cole parameters were determined at discrete temperatures in the vicinity of the glass transition for each of the dielectric data sets. These fits are represented by the full curves shown in *Figure 5*.

The difference between the limiting values in dielectric constant is defined as the dielectric relaxation intensity, $\Delta\epsilon = \epsilon_R - \epsilon_U$, and reflects the population of polymer chain dipoles participating in the glass–rubber relaxation at a given temperature (i.e. the orientational polarizability of the material). The dielectric relaxation intensity for amorphous PEKK 70/30 and for the various crystallized samples is plotted *versus* temperature in *Figure 6*. The relaxation intensity of the amorphous sample is strongly temperature-dependent, with $\Delta\epsilon$ decreasing with increasing temperature and approaching a plateau value prior to the onset of cold crystallization; these data are very similar to results obtained for amorphous PPS[15,16] and PEEK[8,9]. The relaxation intensities of the crystallized samples are smaller than those measured for their amorphous counterpart, as a significant portion of the responding dipoles have been immobilized by the crystalline phase. For samples prepared under more-restrictive crystallization conditions (cold crystallization at 200–275°C), the dielectric relaxation intensity is observed to increase gradually with increasing temperature. For samples crystallized under less-restrictive conditions (cold, melt crystallization at 300°C), $\Delta\epsilon$ is independent of temperature.

In order to quantify the relative population of amorphous-phase dipoles participating in the glass–rubber relaxation at a given temperature, the dielectric mobile-amorphous-phase fraction is defined:

$$W'_{MA} = \Delta\epsilon^{SC}(T)/\Delta\epsilon^{A}(T) \quad (4)$$

where $\Delta\epsilon^{SC}(T)$ is the measured relaxation intensity of the semicrystalline sample, and $\Delta\epsilon^{A}(T)$ is the relaxation intensity of the wholly amorphous specimen evaluated at the same temperature. This expression is completely analogous to the definition of mobile-amorphous-phase

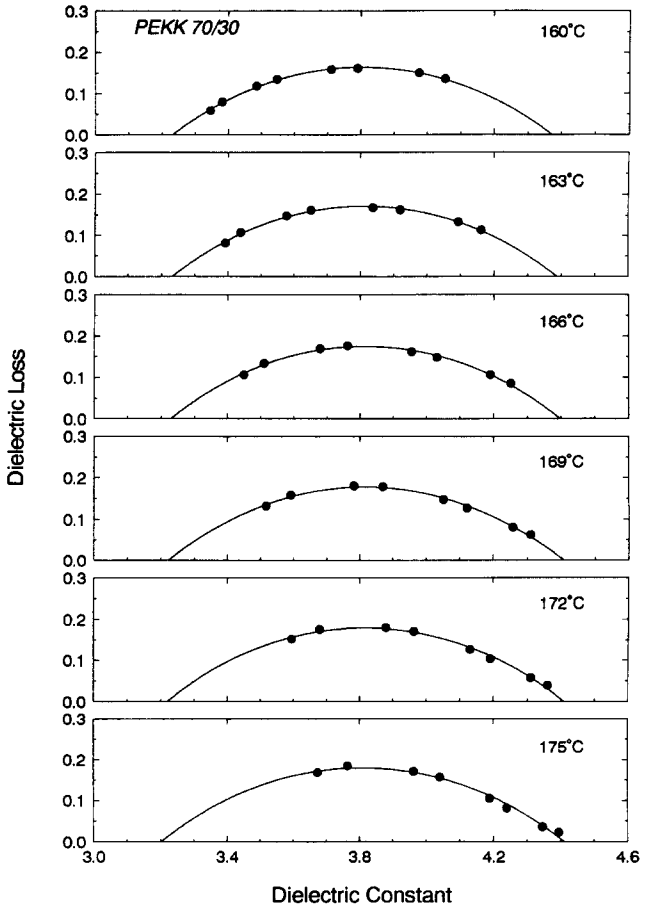

Figure 5 Argand plots for PEKK 70/30 copolymer cold crystallized at 250°C. Glass–rubber (α) relaxation. Semicircular arcs represent least-squares fits to the Cole–Cole equation

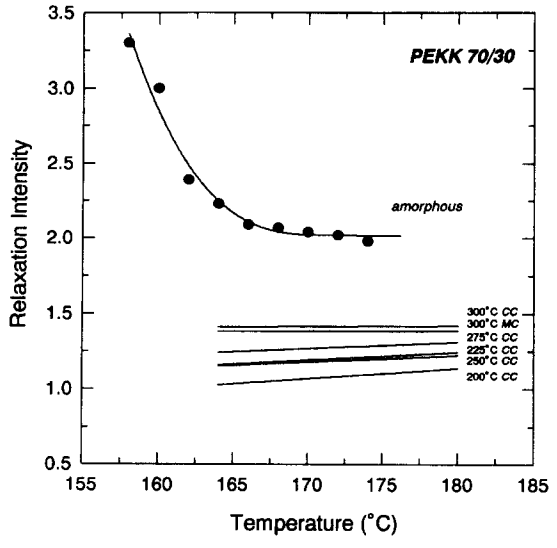

Figure 6 Dielectric relaxation intensity, $\Delta\epsilon = \epsilon_R - \epsilon_U$, vs. temperature (°C) for PEKK 70/30 copolymer. Wholly amorphous material (●) and samples cold crystallized (CC) or melt crystallized (MC) at temperatures indicated

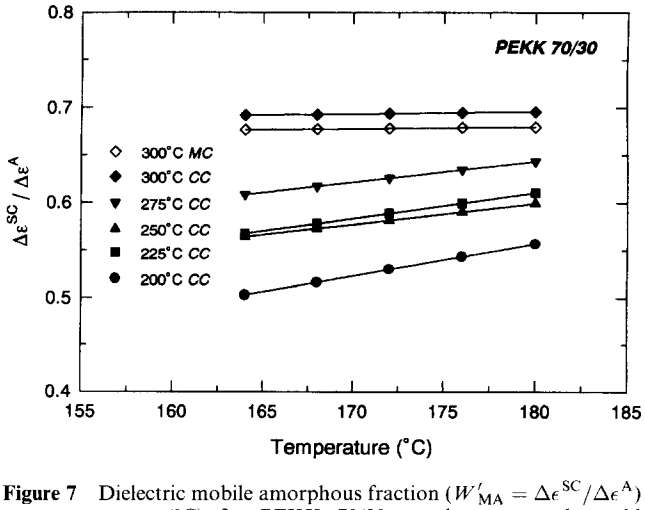

Figure 7 Dielectric mobile amorphous fraction ($W'_{MA} = \Delta\epsilon^{SC}/\Delta\epsilon^{A}$) vs. temperature (°C) for PEKK 70/30 copolymer; samples cold crystallized (CC) or melt crystallized (MC) at temperatures indicated. Symbols: (●) 200°C, CC; (■) 225°C, CC; (▲) 250°C, CC; (▼) 275°C, CC; (◆) 300°C, CC; (◇) 300°C, MC

fraction based on the normalized increase in heat capacity as described above. (W'_{MA} has also been designated as the parameter $\beta(T)$ by previous investigators[8,15,28].) The dielectric mobile-amorphous-phase fraction for the crystallized PEKK 70/30 samples is plotted *versus* temperature in *Figure 7*; $\Delta\epsilon^A$ was taken to be 2.04, independent of temperature. For those samples cold crystallized at lower temperatures, a systematic increase in mobile amorphous fraction with increasing temperature is observed. Comparison of the values of W'_{MA} reported in *Figure 7* with the degree of crystallinity present in these samples (W_C, refer to *Table 2*) shows that the amorphous phase is not fully mobilized across this temperature range. Thus, the increase in W'_{MA} that is observed with temperature is most likely due to the progressive mobilization of the rigid amorphous phase, as has been reported previously for the PPS[15,16] and PEEK[8,9] homopolymers. The quantity of rigid amorphous material in these samples decreases with increasing crystallization temperature. The dielectric data suggest that those copolymer specimens crystallized at higher temperatures (300°C) are fully mobilized above T_g, with W'_{MA} independent of temperature. This result is consistent with dielectric data obtained for PPS copolymer samples containing 8 and 10% *meta*-phenylene linkages[16], and shows that the presence of isophthalate moieties in the backbone of these semiflexible polymers can lead to the complete disruption of the rigid amorphous fraction for less-restrictive crystallization conditions, in agreement with the calorimetric data presented above. Analogous results were recently reported for a semicrystalline polyimide thermoplastic containing *meta* linkages in the chain backbone for improved processability (NEW-TPI)[29,30]. The presence of crystallinity had only a minor effect on the measured glass transition temperature of NEW-TPI, and only a small rigid-amorphous-phase fraction was observed ($W_{RAP} \sim 0.10$ to 0.15). Dielectric measurements on cold-crystallized samples indicated virtually full mobilization of the non-crystalline material at temperatures above T_g. These results again demonstrate the apparent disrupting influence of kinked (1,3-connected) chain segments on the constraint imposed by the crystals on the amorphous phase.

CONCLUSIONS

The glass transition characteristics of poly(aryl ether ketone ketone) have been investigated as a function of polymer backbone structure and thermal history. The glass transition properties of the PEKK 100/0 (T/I) homopolymer were consistent with those reported for other all-*para* semiflexible thermoplastics such as PPS and PEEK. The presence of crystallinity led to an offset in the calorimetric glass transition temperature of as much as 20°C in the crystallized homopolymer samples as compared to the quenched amorphous material owing to the constraint imposed by the crystalline phase on amorphous motions; this was accompanied by a sizeable rigid-amorphous-phase fraction. For the PEKK copolymers, the degree of constraint imposed by the crystalline phase was significantly reduced as compared to the homopolymer, with very little offset in glass transition temperature observed for the crystallized specimens. The measured rigid-amorphous-phase fraction in the copolymers was smaller as compared to the homopolymer, and samples crystallized at higher temperatures displayed virtually full mobilization of all non-crystalline material at temperatures above T_g. These studies thus demonstrate the sensitivity of the glass transition characteristics of the PEKK polymers to crystalline morphology as influenced by polymer backbone structure. The presence of 1,3-connected isophthalate linkages in the copolymers has a strong disrupting influence on the persistence of order into the amorphous phase as manifested by both the minor impact of crystallinity on T_g and the ultimate disappearance of rigid-amorphous-phase fraction. This appears to be a general phenomenon for semiflexible thermoplastics, as similar results have been observed for PPS copolymers that incorporate *meta*-phenylene linkages in the chain backbone, for example, as well as for the NEW-TPI polyimide.

ACKNOWLEDGEMENTS

We are pleased to acknowledge Dr Benjamin Hsiao at DuPont Central Research and Development for providing the polymer samples used in this work.

REFERENCES

1 Boyd, R. H. *Polymer* 1985, **26,** 323
2 Coburn, J. C. and Boyd, R. H. *Macromolecules* 1986, **19,** 2238
3 Illers, K. H. and Breuer, H. *J. Colloid Sci.* 1963, **18,** 1
4 Cheng, S. Z. D., Wu, Z. Q. and Wunderlich, B. *Macromolecules* 1987, **20,** 2802
5 Huo, P. and Cebe, P. *Colloid Polym. Sci.* 1992, **270,** 840
6 Wu, S. S., Kalika, D. S., Lamonte, R. R. and Makhija, S. *J. Macromol. Sci., Phys. Edn* 1996, **B35,** 157
7 Cheng, S. Z. D., Cao, M. Y. and Wunderlich, B. *Macromolecules* 1986, **19,** 1868
8 Huo, P. and Cebe, P. *Macromolecules* 1992, **25,** 902
9 Kalika, D. S. and Krishnaswamy, R. K. *Macromolecules* 1993, **26,** 4252
10 Krishnaswamy, R. K. and Kalika, D. S. *Polymer* 1994, **35,** 1157
11 Jonas, A. and Legras, R. *Macromolecules* 1993, **26,** 813
12 Suzuki, H., Grebowicz, J. and Wunderlich, B. *Makromol. Chem.* 1985, **186,** 1109
13 Suzuki, H. and Wunderlich, B. *Br. Polym. J.* 1985, **17,** 1
14 Grebowicz, J., Lau, S.-F. and Wunderlich, B. *J. Polym. Sci., Polym. Symp.* 1984, **71,** 19
15 Huo, P. and Cebe, P. *J. Polym. Sci., Polym. Phys. Edn.* 1992, **30,** 239
16 Kalika, D. S., Wu, S. S., Lamonte, R. R. and Makhija, S. *J. Macromol. Sci., Phys. Edn* 1996, **B35,** 179
17 Campbell, R. W. and Scoggins, L. E., US Patent No. 3869434, 1975
18 Gardner, K. H., Hsiao, B. S., Matheson, R. R. and Wood, B. A. *Polymer* 1992, **33,** 2483
19 Gardner, K. H., Hsiao, B. S. and Faron, K. L. *Polymer* 1994, **35,** 2290
20 Ho, R.-M., Cheng, S. Z. D., Hsiao, B. S. and Gardner, K. H. *Macromolecules* 1994, **27,** 2136
21 Ho, R.-M., Cheng, S. Z. D., Fisher, H. P., Eby, R., Hsiao, B. S. and Gardner, K. H. *Macromolecules* 1994, **27,** 5787
22 Ho, R.-M., Cheng, S. Z. D., Hsiao, B. S. and Gardner, K. H. *Macromolecules* 1995, **28,** 1938
23 Blundell, D. J. and Newton, A. B. *Polymer* 1991, **32,** 308
24 Kalika, D. S. and Yoon, D. Y. *Macromolecules* 1991, **24,** 3404
25 Ferry, J. D. 'Viscoelastic Properties of Polymers', Wiley, New York, 1980
26 Havriliak, S. and Negami, S. *J. Polym. Sci. (C)* 1966, **14,** 99
27 Cole, R. H. and Cole, K. S. *J. Chem. Phys.* 1941, **9,** 341
28 Schick, C. and Nedbal, J. *Prog. Colloid Polym. Sci.* 1988, **78,** 8
29 Huo, P. P. and Cebe, P. *Polymer* 1993, **34,** 696
30 Huo, P. P., Friler, J. B. and Cebe, P. *Polymer* 1993, **34,** 4387